

Cell size trade-offs govern light exploitation strategies in marine phytoplankton

Tim Key,^{1†} Avery McCarthy,¹ Douglas A. Campbell,^{1*} Christophe Six,^{1†} Suzanne Roy² and Zoe V. Finkel¹

¹*Environmental Science and Biology, Mount Allison University, Sackville, New Brunswick, Canada E4L 1G7.*

²*Institut des Sciences de la Mer, Université du Québec à Rimouski, 310 Allée des Ursulines, Rimouski, Quebec, Canada G5L 3A1.*

Summary

Marine phytoplankton show complex community structures and biogeographic distributions, the net results of physiological and ecological trade-offs of species responses to fluctuating, heterogeneous environments. We analysed photosynthesis, responses to variable light and macromolecular allocations across a size panel of marine centric diatoms. The diatoms have strong capacities to withstand and exploit fluctuating light, when compared with picophytoplankton. Within marine diatoms, small species show larger effective cross-sections for photochemistry, and fast metabolic repair of photosystem II after photoinactivation. In contrast, large diatoms show lower susceptibility to photoinactivation, and therefore incur lower costs to endure short-term exposures to high light, especially under conditions that limit metabolic rates. This size scaling of key photo-physiological parameters thus helps explain the relative competitive advantages of larger versus smaller species under different environmental regimes, with implications for the function of the biogenic carbon pump. These results provide a mechanistic framework to explain and predict shifts in marine phytoplankton community size structure with changes in surface irradiance and mixed layer depth.

Introduction

Diatoms are a diverse group of eukaryotic phytoplankton that significantly contribute to primary production, biogeochemical cycling and to the export of carbon to the

deep ocean (Alldredge and Gotschalk, 1989; Goldman, 1992; Treguer *et al.*, 1995; Smetacek, 1999). The diatoms range in size across species from ~2 µm to a few mm, giving a > 8 order of magnitude range in cell volumes, a wider range than found in other major phytoplankton functional groups such as coccolithophorids, prokaryotic or eukaryotic picophytoplankton (Beardall *et al.*, 2009). This large size range has important implications for the ecology and photophysiology of diatoms versus other phytoplankton.

From bacteria to large mammals, metabolic processes show predictable scaling with organism size (V):

$$\text{Log } M = a + b \text{Log } V - E/kT \quad (1)$$

where M is the metabolic rate, a is the size-normalized metabolic rate, which varies among taxonomic groups (Irwin *et al.*, 2006; Raven *et al.*, 2006), E is the activation energy for metabolism, k is the Boltzmann's constant (8.62 eV K⁻¹), T is temperature and b is the size scaling exponent, measured as the log-log slope of metabolic rate per cell as a function of cell volume (Kleiber, 1947; Hemmingsen, 1960; Peters, 1983; Gillooly *et al.*, 2001). The size scaling exponent b would equal 1 if metabolism scaled in direct proportion to organism size. Instead, under optimal conditions many metabolic processes scale with only a 3/4 exponent with cell volume or mass (Peters, 1983; Gillooly *et al.*, 2001), so that on a per volume or per biomass basis, small cells have higher metabolic rates. This suggests that small species should out-compete similar larger species (Grover, 1989), and indeed, small phytoplankton do tend to numerically dominate communities under stable, oligotrophic environments, probably through their lower nutrient requirements and their higher rates of nutrient diffusion (Munk and Riley, 1952; Chisholm, 1992; Li, 2002). Yet the size of phytoplankton in communities varies over ecological and evolutionary scales (Finkel *et al.*, 2005; 2007; 2009; Irwin *et al.*, 2006), with communities dominated by larger diatoms often found in regions of upwelling and variable environmental conditions (Chisholm, 1992; Li, 2002). Shifts in community structure from small cells towards large diatoms have cascading effects on higher trophic levels, on carbon biogeochemistry and on the biogenic carbon pump (Laws *et al.*, 2000; Kudela *et al.*, 2006). The ecophysiological mechanisms proposed for recurring dominance of communities by large diatoms in coastal areas include their

Received 11 May, 2009; accepted 26 July, 2009. *For correspondence. E-mail dcampbell@mta.ca; Tel. (+1) 506 364 2364; Fax (+1) 506 364 2505. Present addresses: [†]Université Paris VI and CNRS, UMR 7144, Station Biologique, BP74 Place George Teissier, 29680 Roscoff, France; [‡]Department of Microbiology and Immunology, Dalhousie University, Halifax, Nova Scotia, Canada B3H 1X5.

Table 1. Diatom cell size estimations.

Species	Method	Volume (μm^3)	SE	Replicates	Cells
<i>Coscinodiscus wailesii</i> CCMP2513 ^a	Microscopy	2.13E + 07	2.04E + 06	30	30
<i>Coscinodiscus</i> sp. CCMP1583 ^b	Microscopy	4.62E + 05	6.41E + 03	85	85
<i>Coscinodiscus radiatus</i> CCMP312	Microscopy	1.38E + 05	6.15E + 03	56	56
<i>Coscinodiscus</i> sp. CCMP2063	Coulter Counter	3.87E + 03	2.90E + 01	32	11 153
<i>Thalassiosira weissflogii</i> CCMP1010	Coulter Counter	8.01E + 02	6.48E + 00	76	282 584
<i>Thalassiosira pseudonana</i> CCMP1335	Coulter Counter	3.92E + 01	4.45E + 00	25	1 385 856
<i>T. pseudonana</i> CCMP1014	Coulter Counter	1.19E + 01	6.03E-01	10	156 187

a. Cell height equals diameter; <http://starcentral.mbl.edu/mv/portal.php?pagetitle=taxonfactsheet&type=organism&taxon=Coscinodiscus+wailesii>

b. Cell height determined from ratio of height to diameter (Finkel, 2001).

relatively high nutrient uptake capacities and growth rates (Irwin *et al.*, 2006; Raven *et al.*, 2006), capacities for excitation dissipation (Lavaud *et al.*, 2007) and their nutrient storage vacuoles that can provide a growth advantage over smaller cells under pulsed nutrient supply regimes (Sicko-Goad *et al.*, 1984; Raven, 1987; Grover, 1991). Predation, parasitism, viruses and other trophic interactions could also regulate the size structure of phytoplankton communities in favour of large diatoms (Smetacek, 1985; 2001; Raven and Waite, 2004; Thingstad *et al.*, 2005).

All phytoplankton require light for growth, and the variable light regimes imposed by mixing may explain niche partitioning (Litchman, 2000; Litchman and Klausmeier, 2001; Lavaud *et al.*, 2007; Six *et al.*, 2007) and the size structure of phytoplankton communities (Karentz *et al.*, 1991; Raven and Kubler, 2002; Finkel *et al.*, 2009). All oxygenic photoautotrophs suffer photoinactivation of their photosystem II (PSII) complexes through multiple mechanisms (Hakala *et al.*, 2005; Nishiyama *et al.*, 2006; Sarvikas *et al.*, 2006). Under the blue-dominated light prevailing in marine phytoplankton habitats, a single-hit photoinactivation of a target within PSII can largely explain observed patterns of photoinactivation (Nagy *et al.*, 1995; Sinclair *et al.*, 1996; Nishiyama *et al.*, 2006; Six *et al.*, 2007; Tyystjärvi, 2008), but see Janknegt and colleagues (2009). To maintain photosynthesis, phytoplankton must then metabolically remove (Silva *et al.*, 2003) and replace the photoinactivated proteins, particularly the PsbA (D1) subunit of PSII (Aro *et al.*, 1993; Sakurai *et al.*, 2003; Nishiyama *et al.*, 2005; Murata *et al.*, 2007). When the rate of photoinactivation of the PsbA protein exceeds the rate for metabolic replacement of damaged PsbA, the cell suffers net photo-inhibition (Murata *et al.*, 2007) resulting in a decrease in photosynthetic capacity, and potentially to cell death (Janknegt *et al.*, 2009) if the photo-inhibition is sustained.

If cellular pigment concentrations are constant, the efficacy of light absorption by cellular pigment decreases with increasing cell size, due to pigment self-shading (Kirk, 1976; Morel and Bricaud, 1981; Finkel, 2001). Conversely, the same biophysical self-shading renders large

cells less susceptible to ultraviolet radiation damage (Raven, 1984; 1991; Karentz *et al.*, 1991; Garcia-Pichel, 1994; Raven and Kubler, 2002). We test the hypothesis that PSII photoinactivation depends on cell size through a negative size scaling of the susceptibility to photoinactivation, parameterized as an effective cross-section (Nagy *et al.*, 1995; Sinclair *et al.*, 1996), termed σ_i (Six *et al.*, 2007). As a metabolic process, the counteracting PSII repair rate should also depend on cell size. We therefore analysed the photophysiology of a panel of seven centric marine diatoms from the genera *Thalassiosira* and *Coscinodiscus* and compared their responses with those of picocyanobacteria (Six *et al.*, 2007). The study diatom species were derived from warm to temperate waters and have broadly similar, simple centric morphologies but span cell volumes from $\sim 10^1$ to $10^8 \mu\text{m}^3$ (Table 1). We analysed their comparative capacities and mechanisms for light harvesting and PSII repair in response to a moderate upward fluctuation in light and show that cell size imposes inherent trade-offs among the effective absorbance cross-section for light-harvesting σ_{PSII} , the functional cross-section for photoinactivation σ_i , and the metabolic PSII repair rate that counters photoinactivation. Our results contribute size-dependent parameters to model phytoplankton community size structure under different irradiances and mixed layer regimes, and help explain the persistence and success of large diatoms in variable environments.

Results

Cell size scaling of the PSII Antenna (σ_{PSII}) in marine diatoms

Across the size panel of centric diatoms (Table 1) Chl *a* per cell increases with cell volume with a log-log slope of only 0.54 ± 0.02 , $r^2 = 0.96$. As this slope is lower than 1, larger cells contain lower intracellular concentrations of chl *a* than small cells (Fig. 1A). In contrast, PsbA per cell, a proxy for PSII content (Burns *et al.*, 2006), increases with cell volume with a higher log-log slope of 0.80 ± 0.03 , $r^2 = 0.97$ (Fig. 1B). Furthermore, PsbA per

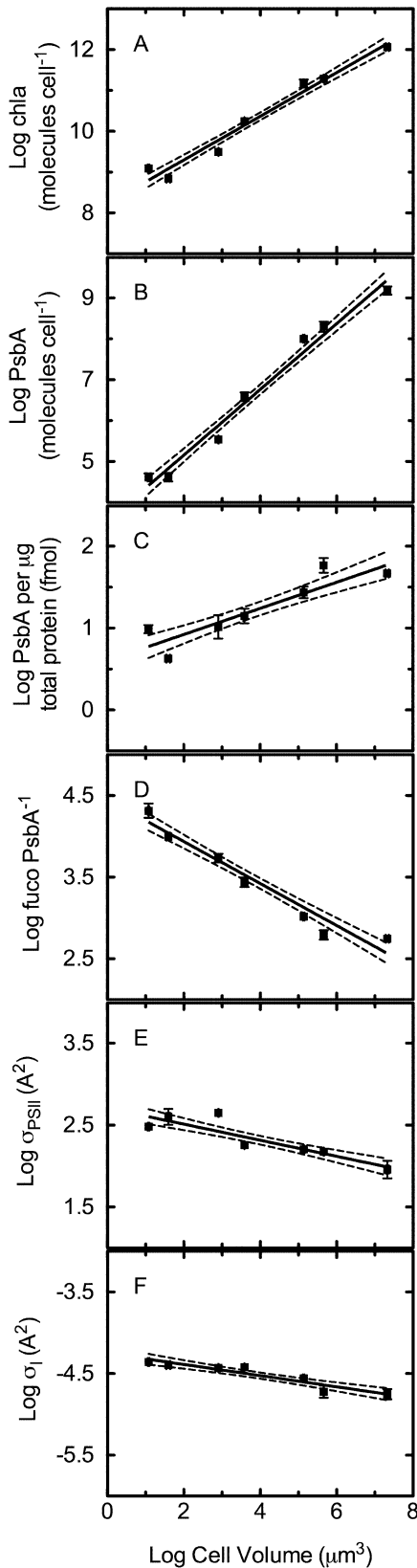


Fig. 1 Cell size dependencies of photosynthetic architecture and function, for a panel of seven centric diatoms.

A. Cellular chl *a* (molecules cell⁻¹).

B. Cellular PSII (PsbA molecules cell⁻¹; a molecular proxy for PSII content).

C. PSII per total protein (PsbA molecules μg total protein⁻¹; a measure of the proportion of total protein allocated to PSII).

D. Fucoxanthin per PSII (Fucoxanthin PsbA⁻¹; a measure of the structural antenna size per PSII).

E. Effective absorbance cross-section for PSII photochemistry, σ_{PSII} (Å²).

F. Functional cross-section for photoinactivation of PSII, σ_i (Å²).

Averages for each species plotted, $n = 4$, \pm SE. All measures were performed on cells from mid-exponential growth phase. Each data set was fit with a log-log regression model versus cell volume.

Dashed lines indicate 95% CI intervals for the regression slopes.

μg total protein increases with cell size (Fig. 1C). The ratio of the antenna pigment fucoxanthin per PsbA (Fig. 1D) decreases with cell size. The level of fucoxanthin per Chl *a* shows no significant change across the range of cell sizes (Table 2), while two forms of chl *c* show opposing trends (Table 2). Larger cells thus have overall lower intracellular pigment concentrations, but allocate a larger proportion of their total cellular protein to their PSII reaction centres (Fig. 1, Table 2). Together, these data suggest smaller structural antennae per PSII reaction centre. These changes in molecular allocations can then explain the negative size scaling of the effective absorbance cross-section for PSII photochemistry, σ_{PSII} , log-log slope of -0.098 ± 0.013 , $r^2 = 0.67$, with cell volume (Fig. 1E).

Cell size scaling of the functional target size for photoinactivation of PSII (σ_i)

The functional cross-section for photoinactivation of PSII σ_i , is estimated as the exponential decay of F_w/F_M plotted versus cumulative photons dose per area, in cells with the counteracting PSII repair blocked by lincomycin, an inhibitor of chloroplast translation (Fig. 2). The magnitude of σ_i is negatively correlated with cell volume with a log-log slope of -0.069 ± 0.009 , $r^2 = 0.66$, indicating that PSII in larger cells is less susceptible to photoinactivation, when assessed on the basis of incident photons (Fig. 1F). The σ_{PSII} and σ_i values for the smallest diatoms are both smaller than those found in picocyanobacteria grown under similar environmental conditions (Table 3).

Cell size scaling of PSII electron transport and repair rate

The PSII electron transport rate ($e^- s^{-1} cell^{-1}$) estimated at $450 \mu\text{mol photons m}^{-2} s^{-1}$ scales with cell volume, with a log-log slope of 0.72 ± 0.04 , $r^2 = 0.95$ (Fig. 3A). This is consistent (within 2 SE) with both the size scaling of growth rate reported for diatoms grown under light-limited conditions (Finkel, 2001), and also with size

Table 2. Size scaling of the photophysiological parameters (log photophysiological parameter = $a + b \cdot \text{Log } V$).

Parameter	Biological significance	a	SE	b	SE	r^2
Macromolecular composition						
$\mu\text{g protein cell}^{-1}$	Index of metabolically active material per cell	-5.8	0.1	0.64	0.02	0.97
Molecules chl $a \mu\text{g protein}^{-1}$	Index of light capture per metabolically active material	14.07	0.09	-0.11	0.02	0.55
fmol PsbA $\mu\text{g protein}^{-1}$	Allocation of protein resource to PSII	0.60	0.09	0.16	0.02	0.70
fmol PsaC $\mu\text{g protein}^{-1}$	Allocation of protein resource to PSI	1.00	0.06	0.14	0.01	0.79
fmol RbcL $\mu\text{g protein}^{-1}$	Allocation of protein resource to RUBISCO	1.3	0.1	0.16	0.03	0.61
Fucoxanthin chl a^{-1}	Ratio of representative antenna pigment to chl a	-0.20	0.02	0.009	0.004	0.17
chl $c1$ chl a^{-1}	Ratio of representative antenna pigment to chl a	-0.99	0.03	-0.024	0.006	0.38
chl $c2$ chl a^{-1}	Ratio of representative antenna pigment to chl a	-1.36	0.04	0.069	0.006	0.73
Metabolic rates						
$R_{\text{PSII}} (\text{s}^{-1})$	Repair rate for PSII	-3.6	0.1	-0.18	0.03	0.58
$R_{\text{PSII}} (\text{PSII s}^{-1} \mu\text{g protein}^{-1})$	Repair for total pool of PSII relative to total protein	5.7	0.2	-0.01	0.04	0.003
PSII ETR ($\text{e}^{-} \text{s}^{-1} \text{PSII}^{-1}$)	Photochemical electron transport per PSII centre	2.60	0.07	-0.08	0.02	0.48
PSII ETR ($\text{e}^{-} \text{s}^{-1} \mu\text{g protein}^{-1}$)	Photochemical PSII electron transport per total protein	3.2	0.1	0.08	0.02	0.33
Photophysics						
$\sigma_{\text{PSII}} (\text{\AA}^2 \text{PSII}^{-1})$	Effective absorbance cross-section for photochemistry per PSII centre	2.71	0.06	-0.10	0.01	0.67
$\sigma_i (\text{\AA}^2 \text{cell}^{-1})$	Effective absorbance cross-section for photochemistry per cell	6.3	0.1	0.70	0.03	0.96
$\sigma_i (\text{\AA}^2 \text{PSII}^{-1})$	Functional absorbance cross for photoinactivation per PSII centre	-4.25	0.04	-0.069	0.009	0.66
$\sigma_i (\text{\AA}^2 \text{cell}^{-1})$	Functional absorbance cross for photoinactivation per cell	-0.7	0.1	0.74	0.03	0.96

scaling of maximum metabolic rates reported for phytoplankton (López-Urrutia *et al.*, 2006). We estimated the maximum inducible rate for the PSII repair cycle (R_{PSII} , PSII $\text{s}^{-1} \text{cell}^{-1}$) for cells grown at low light and then exposed to a 10–15 \times upward light fluctuation, as the difference between the exponential decay rate for F_V/F_M in cells with continuing PSII repair (no lincomycin) and cells in which PSII repair was blocked through addition of lincomycin, an inhibitor of chloroplast translation (Fig. 4). R_{PSII} per cell is correlated with cell volume, but with a log-log slope of only 0.64 ± 0.045 , $r^2 = 0.89$ (Fig. 3B).

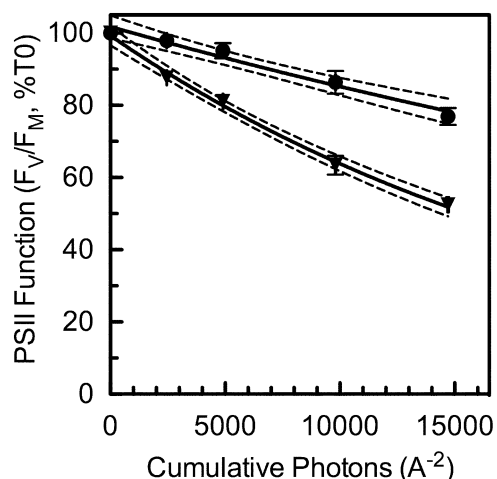


Fig. 2. Response of PSII maximum photochemical yield (F_V/F_M , %T0) as a function of cumulative photon dose (photon m^{-2}) for representative small- and large-diatom species. We fit the data with an exponential decay function, and took the exponent as σ_i , the functional cross-section for photoinactivation of PSII, expressed with units of \AA^2 . Dashed lines indicate 95% CI intervals for the regression curves. Triangles: *Thalassiosira pseudonana* CCMP1014, cell volume $1.19 \times 10^1 \mu\text{m}^3$. Circles: *Coscinodiscus wailiesii* CCMP2513, cell volume $2.13 \times 10^7 \mu\text{m}^3$. $n = 4$, \pm SE.

The size scaling of photosynthetic electron transport and repair rate indicate that small cells have greater metabolic capacity for photosynthesis and PSII repair per unit of cell volume or total biomass (Table 2).

Cell size alters net responses to light fluctuations

Photo-inhibition occurs when the rate of PSII photoinactivation exceeds repair. All of the species examined suffered some net photo-inhibition upon a 10–15 \times increase in light. The smaller centric diatoms such as *Thalassiosira pseudonana* CCMP1335 were able to largely counter the effect of the increased light if PSII repair was allowed to

Table 3. Comparisons of PSII repair rates and the effective target sizes for PSII light harvesting and photoinactivation, among *Prochlorococcus*, marine *Synechococcus* (Six *et al.*, 2007), and small and large marine diatoms.

Taxa	$R_{\text{PSII}} (\text{PSII s}^{-1})$	$\sigma_{\text{PSII}} (\text{\AA}^2 \text{PSII}^{-1})$	$\sigma_i (\text{\AA}^2 \text{PSII}^{-1})$
<i>Prochlorococcus</i> ^a	$1-5 \times 10^{-5}$	460–630	9×10^{-5}
<i>Synechococcus</i> ^b	$10-13 \times 10^{-5}$	380–550	$5-11 \times 10^{-5}$
Small diatoms ^c	12×10^{-5}	300–430	4×10^{-5}
Large diatoms ^d	$2-3 \times 10^{-5}$	60–100	2×10^{-5}

a. *Prochlorococcus* sp. PCC 9511 Sargasso sea surface strain and SS120 deep water strain (Six *et al.*, 2007).

b. *Synechococcus* spp. RCC307 and WH8102 with phycoerythrin phycobilisomes (Six *et al.*, 2007). *Prochlorococcus* and *Synechococcus* cultures were grown under light and temperature conditions comparable to the diatom cultures grown for this study.

c. Includes *Thalassiosira pseudonana* CCMP1335 and CCMP1014, this study.

d. Includes *Coscinodiscus* CCMP1583 and *C. wailiesii* CCMP2513, this study.

R_{PSII} are for cells grown under low light and then challenged with sufficient light to drive R_{PSII} to a maximum. After sustained growth at higher light, R_{PSII} could increase. σ_{PSII} are for cells grown at low light and dark acclimated for 10 min before measurement.

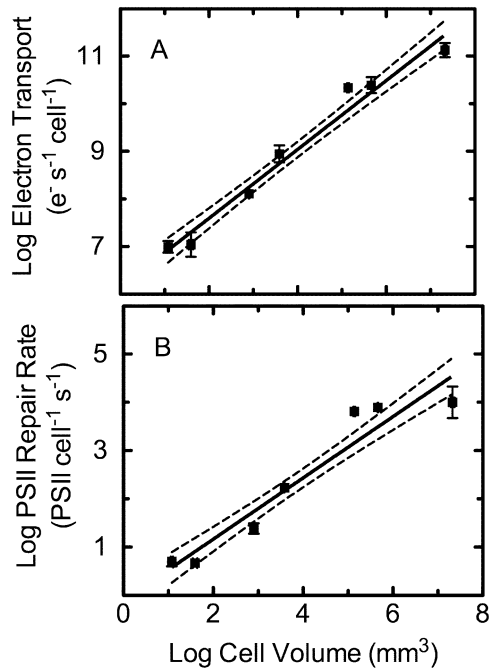


Fig. 3. A. Size dependence of the PSII electron transport rate ($e^- \text{ cell}^{-1} \text{ s}^{-1}$). B. Size-dependence of PSII repair rates ($\text{PSII cell}^{-1} \text{ s}^{-1}$). Averages for each species plotted, $n = 4$, \pm SE. Each data set was fit with a log-log regression model versus cell volume. Dashed lines indicate 95% CI intervals for the regression slopes.

continue (Fig. 4A, open symbols), but when PSII repair was blocked through addition of lincomycin, an inhibitor of chloroplastic translation, the smaller cells suffered rapid photo-inhibition (Fig. 4A, closed symbols). In contrast, the larger centric diatoms such as *Coscinodiscus wailesii* suffered moderate net photo-inhibition in subcultures both with and without lincomycin (Fig. 4B, open symbols) although the cells without lincomycin (Fig. 4B, open symbols) showed greater subsequent recovery than did cells with lincomycin (Fig. 4B, closed symbols).

In the smaller centric diatoms such as *T. pseudonana* CCMP1335 rapid modulations of R_{PSII} (Fig. 5, triangles) can counter the effect of the increased light up to a threshold light level E_{tol} (Six *et al.*, 2007), where R_{PSII} equals the rate of photoinactivation, $E \cdot \sigma_i$ (Fig. 5, dotted line). If, however, the light is held above E_{tol} , or if R_{PSII} were to be restricted by metabolic or environmental factors, the small cells suffer rapid net photo-inhibition because of their high intrinsic susceptibility to photoinactivation (Fig. 5, dotted line). In contrast, in the larger centric diatoms such as *C. wailesii* R_{PSII} is slow (Fig. 5, diamonds). These large cells, however, have lower photoinactivation rates, $E \cdot \sigma_i$ (Fig. 5, dashed line) because their effective target size for photoinactivation, σ_i , is small. Therefore, even with their low R_{PSII} , larger cells suffer only moderate photo-inhibition over a wide range of irradiances. The small centric

diatoms rely heavily on rapidly inducible metabolic PSII repair to counter photoinactivation in response to high light exposure. In contrast, the larger centric diatoms show lower bio-optical susceptibility to photoinactivation and rely less on contemporaneous metabolic PSII repair.

Discussion

The growth of smaller phytoplankton species is often favoured, relative to larger species, due to their higher biomass-normalized metabolic rates, superior rates of light and nutrient acquisition, lower nutrient requirements and slower sinking rates. The frequent abundance of medium to large diatoms in coastal areas is then usually attributed to the size dependencies of loss processes such as grazing (Morin and Fox, 2004; Thingstad *et al.*, 2005). We now find that small cells are more susceptible to photoinactivation of PSII than are large cells, which

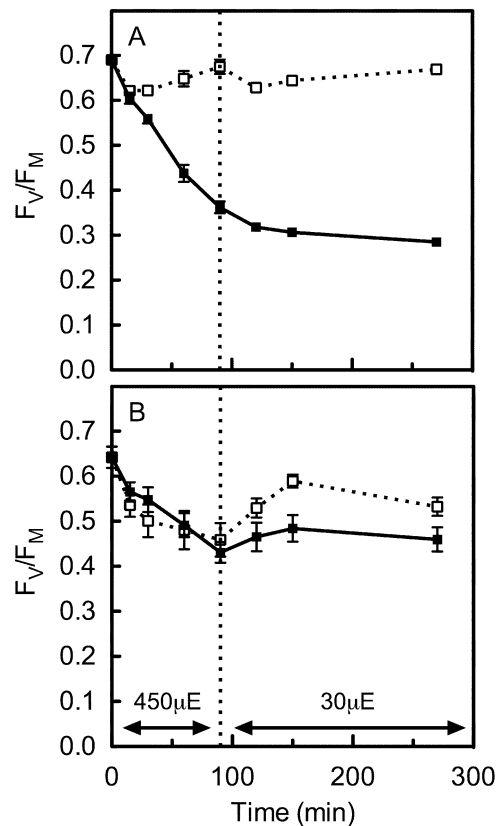


Fig. 4. Responses of PSII maximum photochemical yield (F_v/F_M) versus time.

A. Representative small marine centric diatom *Thalassiosira pseudonana* CCMP1014.

B. Representative large marine centric diatom *Coscinodiscus wailesii* CCMP2513.

Both species were grown at $30 \mu\text{mol photons m}^{-2} \text{ s}^{-1}$, then exposed to $450 \mu\text{mol photons m}^{-2} \text{ s}^{-1}$ for 90 min and then allowed to recover at $30 \mu\text{mol photons m}^{-2} \text{ s}^{-1}$ for 180 min. $n = 4$, \pm SE. Cultures were treated (closed symbols) with the protein synthesis inhibitor lincomycin, or not (open symbols).

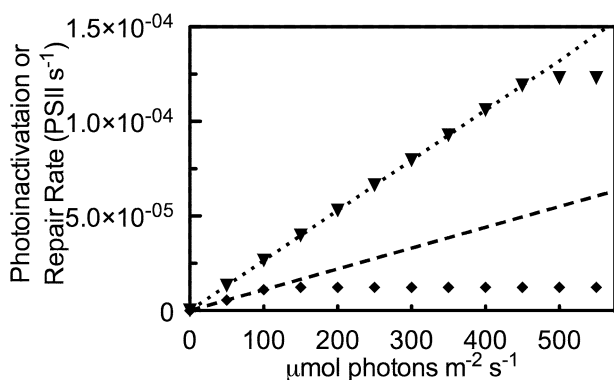


Fig. 5. PSII photoinactivation and repair rates for small and large diatoms. Dotted line: photoinactivation rate modelled as $\sigma_i E$ for *Thalassiosira pseudonana* CCMP1014, cell volume $1.19 \times 10^1 \mu\text{m}^3$, where E is the irradiance expressed in $\mu\text{mol photons m}^{-2} \text{s}^{-1}$. Dashed line: photoinactivation rate modelled for *Coscinodiscus wailesii* CCMP2513, cell volume $2.13 \times 10^7 \mu\text{m}^3$. Triangles: R_{PSII} for *T. pseudonana* CCMP1014, cell volume $1.19 \times 10^1 \mu\text{m}^3$. R_{PSII} was set equal to the magnitude of the modelled photoinactivation rate up to E_{tol} , the light level at which photoinactivation rate equals the maximum R_{PSII} . R_{PSII} was then assumed to plateau at higher light levels. Diamonds: R_{PSII} for *C. wailesii* CCMP2513, cell volume $2.13 \times 10^7 \mu\text{m}^3$. $n = 4$, \pm SE.

thereby face lower metabolic costs to respond to fluctuating light. We hypothesize that phytoplankton community transitions from small to large cells, which notably occur from offshore to coastal waters, can be driven by changes in the mixing and light regime (MacIntyre *et al.*, 2000; Bouman *et al.*, 2006; Lavaud *et al.*, 2007), because of the inherent trade-off of higher light harvesting per PSII and higher maximum metabolic rates in smaller cells versus a lower cross-section for photoinactivation of PSII, and lower maximum metabolic rates in larger cells.

The effective absorbance cross-section for PSII, σ_{PSII} , and the number of photosynthetic units determine photosynthetic capacity under light-limiting conditions. High σ_{PSII} are associated with the smallest phytoplankton *Prochlorococcus* and *Synechococcus* spp., and σ_{PSII} decreases with increasing volume within marine diatoms (Table 3; Fig. 1C). The high σ_{PSII} of smaller cells is often attributed to higher pigment-specific absorption relative to larger cells with similar intracellular pigment concentrations. In actuality larger cells tend to have lower cellular pigment concentrations than smaller cells under similar environmental conditions (Agustí, 1991), thereby counteracting the package effect associated with increasing cell size (Finkel *et al.*, 2004). In this study Chl *a* cell⁻¹ scales with volume with a low log-log exponent of 0.54 ± 0.02 (Fig. 1A), which should counteract any package effect associated with increased cell volume (Finkel *et al.*, 2004). Nevertheless, we do observe a negative size scaling of σ_{PSII} (Fig. 1F), which we attribute to the decrease in the structural size of the antennae per reaction centre (Fig. 1D).

The optical constraints that contribute to smaller σ_{PSII} for larger cells can also protect these larger cells from visible and ultraviolet radiation damage (Hakala *et al.*, 2005; Nishiyama *et al.*, 2006; Sarvikas *et al.*, 2006; Six *et al.*, 2007). Functionally, the negative size scaling for σ_i means that larger cells enjoy a lower intrinsic susceptibility to PSII photoinactivation compared with smaller cells (Figs 1F, 2–5), at least for the moderate, blue light shift we applied (for the effects of much higher irradiance see Janknegt *et al.*, 2009). Thus larger cells incur lower metabolic costs for PSII repair to counter their slower rate of photoinactivation at a given light level.

Across the diversity of diatoms, the genes encoding the core photosynthetic complexes are well conserved (Armbrust *et al.*, 2004; Bowler *et al.*, 2008), yet different niches drive adaptations towards distinct macromolecular compositions across this functionally diverse group (Strzepek and Harrison, 2004). Cell size imposes a trade-off between high metabolic rates and PSII light capture versus susceptibility to PSII photoinactivation, leading to different physiological strategies (Figs 4 and 5) and niche partitioning along the cell size axis. Smaller diatoms invest in high intracellular pigment concentrations and large antennae protein complexes that drive rapid electron transport through a limited pool of PSII, to match their high metabolic capacity (Fig. 3A, Table 2). In contrast, large cells have lower total intracellular pigment concentrations and lower antennae to reaction centre ratios, driving lower electron transport per PSII. As a consequence, larger cells allocate a higher proportion of their total protein to PsbA and other photosynthetic complexes than do smaller cells, yet still achieve lower maximum metabolic rates (Fig. 3A; Table 2). Smaller cells will tend to have higher growth rates under most steady-state conditions. Larger cells, however, are buffered (Behrenfeld *et al.*, 1998) through their higher PSII content and lower σ_i against PSII photoinactivation during transient high light episodes (Figs 4 and 5). Thus large cells will suffer less photo-inhibition than small cells, particularly under conditions such as low temperatures where metabolic PSII repair rates are inhibited. Size scaling of σ_{PSII} and σ_i also predicts shifts in the size scaling of growth and photosynthesis with the light regime (Raven, 1991; Finkel, 2001; 2004; Raven and Kubler, 2002; Raven *et al.*, 2006). Future work needs to consider the relative importance of the size-dependent photoinactivation and repair, versus oxidative stress detoxification (Janknegt *et al.*, 2009) and non-photochemical quenching strategies (Lavaud *et al.*, 2004; 2007; Lavaud, 2007; Grouneva *et al.*, 2008) under different combinations of irradiance, temperature and nutrient concentrations.

In comparison with other taxonomic groups, especially the prokaryotic *Prochlorococcus* and *Synechococcus* spp., the diatoms have higher PSII repair rates (Table 3).

These taxonomic differences in the PSII repair rates may be due to differences in the structure and composition of the photosynthetic apparatus, which alter protein clearance and re-assembly (Six *et al.*, 2007). The high PSII repair rates of the diatoms make them well adapted to mixed layer regimes that transiently expose cells to low and high irradiance (MacIntyre *et al.*, 2000). Within the diatoms, PSII electron transport and repair rates are consistent with a 3/4 size scaling of metabolic rate (Fig. 3). The diatom size range best adapted to a given light regime then depends on the trade-off between higher PSII absorption cross-section and repair rates associated with smaller cells versus the lower cross-section for PSII photoinactivation associated with larger cells. A decrease in temperature or other factors that restrain metabolic rates will decrease the repair rate, but will have little effect on σ_i , thereby favouring the net growth and survival of larger cells in response to exposure to fluctuating irradiance. Taxonomic differences in the photosynthetic apparatus (Strzepek and Harrison, 2004) can now be functionally parameterized using σ_i , σ_{PSII} and PSII repair rates to reconcile observed differences in the impacts of ultraviolet and light on phytoplankton community size structure (Karentz *et al.*, 1991; Laurion and Vincent, 1998). These size-dependent parameters contribute a new conceptual framework to understand phytoplankton community size structure under different irradiances and mixed layer regimes.

Experimental procedures

The light challenge approach, methods and data transformations were previously described (Six *et al.*, 2007). All experiments were performed on cultures from mid-exponential phase growth.

Culture conditions and treatments

The diatoms *T. pseudonana* CCMP1014 and CCMP1335, *Thalassiosira weissflogii* CCMP1010, *Coscinodiscus* sp. CCMP2063, *Coscinodiscus* sp. CCMP1583, *Coscinodiscus radiatus* CCMP312 and *C. wailesii* CCMP2513 were maintained in K medium (Keller *et al.*, 1987) in polystyrene flasks (Corning) under continuous 30 $\mu\text{mol photons m}^{-2} \text{s}^{-1}$ (daylight fluorescent tubes, Sylvania) at $22 \pm 1^\circ\text{C}$, with twice daily manual agitation. These species are derived from warm or temperate water and we intentionally excluded temperature as a potentially confounding variable in the experiments.

Mid-exponential cultures were split into two flasks: one was supplemented with 500 $\mu\text{g ml}^{-1}$ lincomycin, and both flasks were incubated in the dark for 10 min, to allow the antibiotic to penetrate the cells and inhibit ribosome function. The two flasks were then shifted for 90 min to 450 $\mu\text{mol photons m}^{-2} \text{s}^{-1}$ blue light (300 for *T. weissflogii* CCMP1010), sufficient to induce detectable photo-inhibition within 15 min of treatment (LEE Filter #183, Panavision; 455–479 nm peak

transmission, 406–529 nm half-height width). Samples were collected at 15, 30, 60 and 90 min to measure biophysical properties and for later protein immunodetection (PsbA from PSII, PsaC from PSI; RbcL from RUBISCO) and pigment analyses. The subcultures were then shifted back to their initial growth light to monitor recovery. One-millilitre samples were fixed with 0.2% glutaraldehyde grade II (Sigma Aldrich) for later determinations of cell numbers and cell sizes.

Chlorophyll fluorescence measurements and data processing

Culture samples were collected during the time-course and dark-adapted inside a temperature-controlled cuvette holder at 22°C . These samples were submitted to a blue-green modulated measuring light (4 Hz; Xenon-PAM, Walz, Effeltrich, Germany) to measure the basal fluorescence level F_0 and a saturating light pulse (4000 $\mu\text{mol photons m}^{-2} \text{s}^{-1}$, 500 ms) was triggered to measure the maximal fluorescence level in the dark F_M . Actinic light was then activated at an irradiance corresponding to the high-light treatment; after 1–3 min for signal stabilization (F_i level), a saturating light pulse was triggered to determine the light-acclimated maximal fluorescence under treatment light (F_M'). Then a short period of dark (2–3 s) was applied in order to measure the basal fluorescence level in light-acclimated sample F_0' . The PSII inhibitor 3-(3,4-dichlorophenyl)-1,1-dimethylurea (DCMU) was then added and after signal stabilization, a light pulse was triggered again to determine the maximal fluorescence in the presence of DCMU $F_{M \text{ DCMU}}$. The photochemical yield of PSII was calculated as: $F_v/F_M = (F_M - F_0)/F_M$. Photochemical quenching was estimated as: $q_p = (F_M' - F_i)/(F_M' - F_0')$, as an index of the instantaneous fraction of PSII centres open for photochemistry.

After the high-light-stress treatment the lincomycin-treated subcultures, particularly in the larger-diatom species, showed some recovery of F_v/F_M levels during the low-light recovery period (Fig. 4). There was no re-accumulation of PsbA protein during the recovery period in the lincomycin-treated subcultures (data not presented). Therefore, the lincomycin was effective at inhibiting protein synthesis. The partial recovery of F_v/F_M in the lincomycin-treated subcultures therefore reflects the relaxation of a kinetic component of non-photochemical quenching induced during the high light stress in some diatoms, which relaxes slowly after the return to low light (Owens, 1986; Caron *et al.*, 1987; Ting and Owens, 1993; Lavaud, 2007). For estimating values for σ_i , the functional cross-section for photoinactivation of PSII (Fig. 2) and R_{PSII} we therefore corrected the F_v/F_M values for the 15, 30, 60 and 90 min high-light treatment points by the magnitude of any recovery of F_v/F_M in the lincomycin-treated subcultures during the subsequent low-light recovery (Fig. 4). We applied this correction to separate photoinactivation of PSII, which cannot recover in the absence of PsbA synthesis, from down-regulation of PSII through slow phases of non-photochemical quenching in diatoms that can relax without protein synthesis. The applied correction largely accounted for the sharp drop in F_v/F_M observed in some species during the first 15 min of high-light treatments (Fig. 4). In any case, this correction had only small effects on estimates of σ_i and R_{PSII} . It should be noted that both σ_i and σ_{PSII} estimates are for blue irradiance,

approximating the spectral light quality in marine environments and predominantly harvested by diatoms. Under other wavelength ranges, σ_i would differ because the absorbance cross-section for photoinactivation is dependent upon wavelength (Cullen *et al.*, 1992; Sarvikas *et al.*, 2006).

The effective absorption cross-section serving PSII photochemistry (σ_{PSII} , nm² PSII⁻¹) (Gorbunov *et al.*, 1999) was determined on a culture sample dark acclimated for 5 min and then exposed to a saturating single turnover flash (blue LED, 455 ± 20 nm; FRe fluorimeter, Satlantic, Halifax, NS, Canada). Values of σ_{PSII} were determined from the fluorescence saturation curves analysed with MATLAB software using the Fireworx program (Barnett, 2007), with instrument specific calibration factors (Satlantic).

The maximum PSII repair rate R_{PSII} was parameterized as the difference of the exponential rates of F_v/F_m decay in the control and lincomycin-treated cultures. Following (Six *et al.*, 2007), we estimated a functional cross-section for PSII photoinactivation (Nagy *et al.*, 1995; Sinclair *et al.*, 1996) termed σ_i (expressed in m² PSII⁻¹), measured in the absence of PSII repair in the presence of lincomycin. The PSII electron transport per cell was estimated as: E (μmol photons m⁻² s⁻¹) × σ_{PSII} (m² PSII⁻¹) × q_p × (PsbA cell⁻¹). This estimate uses PsbA cell⁻¹ as a proxy for the PSII content of the cell (Burns *et al.*, 2006).

Quantitative immunoblotting and pigment analyses

Culture aliquots were filtered onto glass fibre filters (25 mm, Whatman or Milli-Q), which were immediately flash-frozen in liquid nitrogen and stored at -80°C for later pigment analyses or protein analysis by quantitative immunoblotting (Six *et al.*, 2007; Brown *et al.*, 2008). In particular, we quantified molar levels of PsbA, a molecular proxy for PSII content; PsaC, a molecular proxy for PSI content; and RbcL, a molecular proxy for RUBISCO content. Pigments were extracted in methanol, separated using high-performance liquid chromatography (Zapata *et al.*, 2000), and identified and quantified according to their retention time, spectrum and comparison with standards (DHI, <http://c14.dhigroup.com>).

Acknowledgements

We thank Laurel McIntyre for skilled assistance with culture maintenance and Dr Marie Lionard for assistance with pigment analyses.

References

Agustí, S. (1991) Allometric scaling of light absorption and scattering by phytoplankton cells. *Can J Fish Aquat Sci* **48**: 763–767.

Aldredge, A.L., and Gotschalk, C.C. (1989) Direct observations of the mass flocculation of diatom blooms: characteristics, settling velocities and formation of diatom aggregates. *Deep Sea Res* **36**: 159–171.

Armbrust, E.V., Berges, J.A., Bowler, C., Green, B.R., Martinez, D., Putnam, N.H., *et al.* (2004) The genome of the diatom *Thalassiosira pseudonana*: ecology, evolution, and metabolism. *Science* **306**: 79–86.

Aro, E.M., Virgin, I., and Andersson, B. (1993) Photoinhibition of photosystem II. Inactivation, protein damage and turnover. *Biochim Biophys Acta Bioenerg* **1143**: 113–134.

Barnett, A.B. (2007) *Fireworx 1.0.3*. Halifax, NS, Canada: Dalhousie University. [WWW document]. URL <http://sourceforge.net/projects/fireworx>

Beardall, J., Allen, D., Bragg, J., Finkel, Z.V., Flynn, K.J., Quigg, A., *et al.* (2009) Allometry and stoichiometry of unicellular, colonial and multicellular phytoplankton. *New Phytol* **181**: 295–309. 10.1111/j.1469-8137.2008.02660.

Behrenfeld, M.J., Prasil, O., Kolber, Z.S., Babin, M., and Falkowski, P.G. (1998) Compensatory changes in Photosystem II electron turnover rates protect photosynthesis from photoinhibition. *Photosynth Res* **58**: 259–268.

Bouman, H.A., Ulloa, O., Scanlan, D.J., Zwirgmaier, K., Li, W.K.W., Platt, T., *et al.* (2006) Oceanographic basis of the global surface distribution of *Prochlorococcus* ecotypes. *Science* **312**: 918–921.

Bowler, C., Allen, A.E., Badger, J.H., Grimwood, J., Jabbari, K., Kuo, A., *et al.* (2008) The *Phaeodactylum* genome reveals the evolutionary history of diatom genomes. *Nature (London)* **456**: 239–244.

Brown, C.M., MacKinnon, J.D., Cockshutt, A.M., Villareal, T.A., and Campbell, D.A. (2008) Flux capacities and acclimation costs in *Trichodesmium* from the Gulf of Mexico. *Mar Biol* **154**: 413–422.

Burns, R.A., MacKenzie, T.D.B., and Campbell, D.A. (2006) Inorganic carbon repletion constrains steady-state light acclimation in the cyanobacterium *Synechococcus elongatus*. *J Phycol* **42**: 610–621.

Caron, L., Berkaloff, C., Duval, J.-C., and Jupin, H. (1987) Chlorophyll fluorescence transients from the diatom *Phaeodactylum tricorutum*: relative rates of cyclic phosphorylation and chlororespiration. *Photosynth Res* **11**: 131–139.

Chisholm, S.W. (1992) Phytoplankton size. In *Primary Productivity and Biogeochemical Cycles in the Sea*. Falkowski, P.G., and Woodhead, A.D. (eds). New York, NY, USA: Plenum Press, pp. 213–237.

Cullen, J.J., Neale, P.J., and Lesser, M.P. (1992) Biological weighting function for the inhibition of phytoplankton photosynthesis by ultraviolet-radiation. *Science* **0258**: 00646–00650.

Finkel, Z.V. (2001) Light absorption and size scaling of light-limited metabolism in marine diatoms. *Limnol Oceanogr* **46**: 86–94.

Finkel, Z.V., Irwin, A.J., and Schofield, O. (2004) Resource limitation alters the 3/4 size scaling of metabolic rates in phytoplankton. *Mar Ecol Prog Ser* **273**: 269–279.

Finkel, Z.V., Katz, M., Wright, J., Schofield, O., and Falkowski, P. (2005) Climatically driven macroevolutionary patterns in the size of marine diatoms over the Cenozoic. *Proc Natl Acad Sci USA* **102**: 8927–8932.

Finkel, Z.V., Sebbo, J., Feist-Burkhardt, S., Irwin, A.J., Katz, M.E., Schofield, O.M.E., and Falkowski, P.G. (2007) A universal driver of macroevolutionary change in the size of marine phytoplankton over the Cenozoic. *Proc Natl Acad Sci USA* **104**: 20416–20420.

Finkel, Z.V., Vaillancourt, C.-J., Irwin, A.J., Reavie, E.D., and Smol, J.P. (2009) Environmental control of diatom community size structure varies across aquatic ecosystems. *Proc Royal Soc Lond B* **276**: 1627–1634.

- Garcia-Pichel, F. (1994) A model for internal self-shading in planktonic organisms and its implications for the usefulness of ultraviolet sunscreens. *Limnol Oceanogr* **39**: 1704–1717.
- Gillooly, J.F., Brown, J.H., West, G.B., Savage, V.M., and Charnov, E.L. (2001) Effects of size and temperature on metabolic rate. *Science* **293**: 2248–2251.
- Goldman, J.C. (1992) Potential role of large oceanic diatoms in new primary production. *Deep Sea Res* **40**: 159–168.
- Gorbunov, M.Y., Kolber, Z.S., and Falkowski, P.G. (1999) Measuring photosynthetic parameters in individual algal cells by Fast Repetition Rate fluorometry. *Photosynth Res* **62**: 141–153.
- Grouneva, I., Jakob, T., Wilhelm, C., and Goss, R. (2008) A new multicomponent NPQ mechanism in the diatom *Cyclotella meneghiniana*. *Plant Cell Physiol* **49**: 1217–1225.
- Grover, J.P. (1989) Influence of cell shape and size on algal competitive ability. *J Phycol* **25**: 402–405.
- Grover, J.P. (1991) Resource competition in a variable environment: phytoplankton growing according to the variable-internal-stores model. *Am Nat* **138**: 811–835.
- Hakala, M., Tuominen, I., Keranen, M., Tyystjarv, i.T., and Tyystjarvi, E. (2005) Evidence for the role of the oxygen-evolving manganese complex in photoinhibition of Photosystem II. *Biochim Biophys Acta* **1706**: 68–80.
- Hemmingsen, A.M. (1960) Energy metabolism as related to body size and respiratory surfaces, and its evolution. *Rep Steno Mem Hosp* **9**: 15–22.
- Irwin, A.J., Finkel, Z.V., Schofield, O.M.E., and Falkowski, P.G. (2006) Scaling-up from nutrient physiology to the size-structure of phytoplankton communities. *J Plankton Res* **28**: 459–471.
- Janknegt, P., de Graaff, M., van de Poll, W., Visser, R., Rijstenbil, J., and Buma, A. (2009) Short term antioxidative responses of 15 microalgae exposed to excessive irradiance including ultraviolet radiation. *Europ J Phycol*, **44**. Advanced online publication, doi: 10.1080/09670260902943273.
- Karentz, D., Cleaver, J.E., and Mitchell, D.L. (1991) Cell survival characteristics and molecular responses of Antarctic phytoplankton to ultraviolet-B radiation. *J Phycol* **27**: 326–341.
- Keller, M.D., Selvin, R.C., Claus, W., and Guillard, R.R.L. (1987) Media for the culture of oceanic ultraphytoplankton. *J Phycol* **23**: 633–638.
- Kirk, J.T.O. (1976) A theoretical analysis of the contribution of algal cells to the attenuation of light within natural waters. III. Cylindrical and spheroidal cells. *New Phytol* **77**: 341–358.
- Kleiber, M. (1947) Body size and metabolic rate. *Physiol Rev* **27**: 511–541.
- Kudela, R., Cochlan, W., Peterson, T., and Trick, C.G. (2006) Impacts on phytoplankton biomass and productivity in the Pacific Northwest during the warm ocean conditions of 2005. *Geophys Res Lett* **33**: 1–6.
- Laurion, I., and Vincent, W.F. (1998) Cell size versus taxonomic composition as determinants of UV-sensitivity in natural phytoplankton communities. *Limnol Oceanogr* **43**: 1774–1779.
- Lavaud, J. (2007) Fast regulation of photosynthesis in diatoms: mechanisms, evolution and ecophysiology. *Funct Plant Sci Biotech* **1**: 267–287.
- Lavaud, J., Rousseau, B., and Etienne, A.-L. (2004) General features of photoprotection by energy dissipation in planktonic diatoms (Bacillariophyceae). *J Phycol* **40**: 130–137.
- Lavaud, J., Strzepak, R.F., and Kroth, P.G. (2007) Photoprotection capacity differs among diatoms: possible consequences on the spatial distribution of diatoms related to fluctuations in the underwater light climate. *Limnol Oceanogr* **52**: 1188–1194.
- Laws, E.A., Falkowski, P.G., Smith, W.O.J., Ducklow, H., and McCarthy, J.J. (2000) Temperature effects on export production in the open ocean. *Global Biogeochem Cycles* **14**: 1231–1246.
- Li, W.K.W. (2002) Macroecological patterns of phytoplankton in the northwestern North Atlantic Ocean. *Nature* **419**: 154–157.
- Litchman, E. (2000) Growth rates of phytoplankton under fluctuating light. *Freshwater Biol* **44**: 223–235.
- Litchman, E., and Klausmeier, C.A. (2001) Competition of phytoplankton under fluctuating light. *Am Nat* **157**: 170–187.
- López-Urrutia, A., San Martin, E., Harrip, R.P., and Irigoien, X. (2006) Scaling the metabolic balance of the oceans. *Proc Natl Acad Sci USA* **103**: 8739–8744.
- MacIntyre, H.L., Kana, T.M., and Geider, R.J. (2000) The effect of water motion on short-term rates of photosynthesis by marine phytoplankton. *Trends Plant Sci* **5**: 12–17.
- Morel, A., and Bricaud, A. (1981) Theoretical results concerning light absorption in a discrete medium, and application to specific absorption of phytoplankton. *Deep Sea Res* **1**: 28A: 1375–1393.
- Morin, P.J., and Fox, J.W. (2004) Diversity in the deep blue sea. *Nature* **429**: 814.
- Munk, W.H., and Riley, G.A. (1952) Absorption of nutrients by aquatic plants. *J Mar Res* **11**: 215–240.
- Murata, N., Takahashi, S., Nishiyama, Y., and Allakhverdiev, S.I. (2007) Photoinhibition of photosystem II under environmental stress. *Biochim Biophys Acta* **1767**: 1414–1421.
- Nagy, L., Balint, E., Barber, J., Ringler, A., Cook, K.M., and Maroti, P. (1995) Photoinhibition and law of reciprocity in photosynthetic reactions of *Synechocystis* sp PCC6803. *J Plant Physiol* **145**: 410–441.
- Nishiyama, Y., Allakhverdiev, S.I., and Murata, N. (2005) Inhibition of the repair of PSII by oxidative stress in cyanobacteria. *Photosynth Res* **84**: 1–7.
- Nishiyama, Y., Allakhverdiev, S.I., and Murata, N. (2006) A new paradigm for the action of reactive oxygen species in the photoinhibition of photosystem II. *Biochim Biophys Acta* **1757**: 742–749.
- Owens, T.G. (1986) Light-harvesting in the diatom *Phaeodactylum tricornutum* II. Distribution of excitation energy between the photosystems. *Plant Physiol* **80**: 739–746.
- Peters, R.H. (1983) *The Ecological Implications of Body Size*. Cambridge, UK: Cambridge University Press.
- Raven, J.A. (1984) A cost-benefit analysis of photon absorption by photosynthetic unicells. *New Phytol* **98**: 593–625.
- Raven, J.A. (1987) The role of vacuoles. *New Phytol* **106**: 357–422.
- Raven, J.A. (1991) Responses of aquatic photosynthetic organisms to increased solar UVB. *J Photochem Photobiol B Biol* **9**: 239–244.

- Raven, J.A., and Kubler, J.E. (2002) New light on the scaling of metabolic rate with the size of algae. *J Phycol* **38**: 11–16.
- Raven, J.A., and Waite, A.M. (2004) The evolution of silicification in diatoms: inescapable sinking and sinking as escape? *New Phytol* **162**: 45–61.
- Raven, J.A., Finkel, Z.V., and Irwin, A.J. (2006) Picophytoplankton: bottom-up and top-down controls on ecology and evolution. *Vie Milieu* **55**: 209–215.
- Sakurai, I., Hagio, M., Gombos, Z., Tyystjärvi, T., Paakkari, V., Aro, E.-M., and Wada, H. (2003) Requirement of phosphatidylglycerol for maintenance of photosynthetic machinery. *Plant Physiol* **133**: 1376–1384.
- Sarvikas, P., Hakala, M., Patsikka, E., Tyystjärvi, T., and Tyystjärvi, E. (2006) Action spectrum of photoinhibition in leaves of wild type and npq1–2 and npq4–1 mutants of *Arabidopsis thaliana*. *Plant Cell Physiol* **47**: 391–400.
- Sicko-Goad, L.M., Schekske, C.L., and Stoermer, E.F. (1984) Estimation of intracellular carbon and silica content of diatoms from natural assemblages using morphometric techniques. *Limnol Oceanogr* **29**: 1170–1178.
- Silva, P., Thompson, E., Bailey, S., Kruse, O.W., Mullineaux, C., Robinson, C., et al. (2003) FtsH is involved in the early stages of repair of photosystem II in *Synechocystis* sp. PCC 6803. *Plant Cell* **15**: 2152–2164.
- Sinclair, J., Park, Y.I., Chow, W.S., and Anderson, J.M. (1996) Target theory and the photoinactivation of Photosystem II. *Photosynth Res* **50**: 33–40.
- Six, C., Finkel, Z.V., Irwin, A.J., and Campbell, D.A. (2007) Light variability illuminates niche-partitioning among marine picocyanobacteria. *PLoS One* **2**: e1341. 10.1371/journal.pone.0001341.
- Smetacek, V.S. (1985) Role of sinking in diatom life-history cycles: ecological, evolutionary and geological significance. *Mar Biol* **84**: 239–251.
- Smetacek, V. (1999) Diatoms and the ocean carbon cycle. *Protist* **150**: 25–32.
- Smetacek, V. (2001) A watery arms race. *Nature* **411**: 745.
- Strzepek, R.F., and Harrison, P.J. (2004) Photosynthetic architecture differences in coastal and oceanic diatoms. *Nature* **431**: 689–692.
- Thingstad, F., Øvreås, L., Egge, J.K., Løvdal, T., and Heldal, M. (2005) Use of non-limiting substrates to increase size; a generic strategy to simultaneously optimize uptake and minimize predation in pelagic osmotrophs? *Ecol Lett* **8**: 675–682.
- Ting, C.S., and Owens, T.G. (1993) Photochemical and non-photochemical fluorescence quenching processes in the diatom *Phaeodactylum tricornutum*. *Plant Physiol* **101**: 1323–1330.
- Treguer, P., Nelson, D., Vanbennekem, A., DeMaster, D., Leynaert, A., and Queguiner, B. (1995) The silica balance in the world ocean – a reestimate. *Science* **268**: 375–379.
- Tyystjärvi, E. (2008) Photoinhibition of photosystem II and photodamage of the oxygen evolving manganese cluster. *Coor Chem Rev* **252**: 361–376.
- Zapata, M., Rodriguez, F., and Garrido, J.L. (2000) Separation of chlorophylls and carotenoids from marine phytoplankton: a new HPLC method using a reversed phase C₈ column and pyridine-containing mobile phases. *Mar Ecol Prog Ser* **195**: 29–45.